Int J Adv Manuf Technol
DOI 10.1007/s00170-011-3591-0

ORIGINAL ARTICLE

Numerical modeling of the momentum and thermal characteristics of air flow in the intercooler connection hose

Alper Uysal · A. Alper Ozalp · Ayhan Korgavus · Orhan Korgavus

Received: 13 September 2010 / Accepted: 7 June 2011

Abstract This paper presents a numerical investigation on the momentum and thermal characteristics of an intercooler connection hose that is in use in the 1.3 SDE 75 CV type FIAT engine. Computational analyses are carried out with ANSYS FLUENT v.12.0.1, where both stationary and vibrating scenarios are handled. The work is structured in accordance with the "Subsystem Functional Description for Charge Air Hoses Fiat 225 Euro 5" FIAT standard, where the air mass flow rate, temperature, and gage pressure at the hose inlet are identified as $\dot{m}$=0.085 kg/s, T_{in}=90°C, and P_{in}=130 kPa, respectively. In the stationary case, it is determined that the pressure loss value in the air domain of the hose is ΔP_K=1.50 kPa; moreover, the corresponding data for the temperature drop is ΔT=0.80°C. Vibration is characterized by employing simple harmonic motion at the engine side of the hose. The fluid–solid interaction methodology showed that pressure loss values grow due to vibration; moreover, the impact of vibration came out to generate diverse fluctuation schemes at different sections of the hose.

Keywords Engine hose · Momentum and thermal characteristics · Stationary/vibration operation · Fluid–solid interaction

A. Uysal · A. Korgavus · O. Korgavus
Unver Group, Kayapa Industrial Zone,
16315, Nilufer,
Bursa, Turkey

A. A. Ozalp (✉)
Department of Mechanical Engineering, Uludag University,
16059, Gorukle,
Bursa, Turkey
e-mail: aozalp@uludag.edu.tr

1 Introduction

The hose connections in the overall internal combustion engine (ICE) assembly are considered as one of the most safety relevant components in the automobiles. As their responsibility is to transport fluid, in water or gas form, between various ICE parts, they are required to resist different ranges of flow rates, pressures, temperatures, and vibrations. Their durability in extreme operation conditions, harsh environment for a sufficiently long guarantee period is essential for original equipment manufacturers, due to the fact that the fail or poor performance of a single hose can cause significant damages or disqualified prospects in the overall ICE. To satisfy these necessities, the scientific research on hose development covers a broad perspective including the development of a unique hose [1], that is capable of functioning on both the radiator and the manifold, detailing the safety issues regarding the pressure variations during the engine operation [2], investigations on the material definition and geometric design [3] and even in the medicine sector for feasible and ergonomic purposes [4]. Being independent from the primary focus, every hose operation-oriented work is structured on the three main influential parameters of pressure, temperature, and vibration.

Since the presence of pressure and temperature is primarily due to the existence of the fluid action in the hose, their impact and so occurring requirements are considered simultaneously. Kain [5] worked on the stress corrosion cracking of stainless steel hoses under high pressure conditions and reported that the geometric and structural design of the connection ends have a characteristic role on this phenomenon. In a numerical work, Hau and Wang [6] investigated the influences of temperature and pressure anisotropies and the resulting energy dissipations

Published online: 26 August 2011

within the hose geometry. As Friedrichs et al. [7] concentrated on the flow of multi-component chemical mixtures in the hose of a gas controlling device, composite material-based design and manufacture of high-temperature and pressure-durable hose was handled by Ilardo and Williams [8]. Ilgamov and Ratrout [9] evaluated the affects of pressure, flow velocity as well as system weight on the post-buckling behavior of a high-temperature hose. Cronin et al. [10] indicated that the thermo-hydraulic rupture arising from the thermal expansion of liquids is a common fact with flexible elastomer hoses in short lengths and proposed their solution with reverse engineering where the onset of the design phase was the evaluation of the maximum acceptable stress level. Gas ejection from a hot volume in pre-determined flow rates was considered by Rath et al. [11] who determined that the success of the hose design was mainly dependent on the interrelation of the boundary conditions and the critical cross-sectional reduction in the flow direction. Cho et al. [12] pointed out the possibility of excessive radial expansion of hoses due to high temperature and pressure; they carried out a 3-D finite element analysis to propose the application periodic fiber tows to reinforce the complete mechanical properties. In a similar work, Simmons [13] demonstrated the contribution of thermoplastic materials especially in systems with aggressive fluids and abrasion resistance. The complementary research of Stoeckel and Borden [14] aimed to develop an alloy that is capable of satisfying its elastic ability under intense temperature and pressure variations, where the new formula is as well capable of absorbing pressure shocks and system shift due to viscosity change.

Vibration is a frequent event in engineering systems; as engine hoses are also faced with this occurrence, previous research has indicated the necessity of detailing the mechanisms and the corresponding outputs. Marquez et al. [15] pointed out the significance of dynamic loads originating from gas pulsations and investigated the impact of hose flexibility at the discharge side of a compressor. As modes of wave propagation and dispersion relations in a cylindrical annuli was numerically considered by Liu et al. [16], Drew et al. [17] experimented on the longitudinal transmission of pressure fluctuations and structural vibrations in flexible hoses. Nishimura and Matsunaga [18] also worked on the pressure wave propagation in a hydraulic hose and analyzed the interrelation of the pressure perturbation and the simultaneously excited vibration. On the problem of wave propagation, Yu and Kojima [19] carried out a research on the particular case where the flexible hydraulic hose was viscoelastically anisotropic. Drexel and Ginsberg [20] investigated the scenario where the system is irritated with multiple vibration sources with different frequencies; they aimed to enlighten the absorber effect of distinct damping configurations. The concept of impact absorbers was taken as well into consideration by Shaw and Pierre [21]. By foregrounding the important absorber design parameters including mass, coefficient of restitution, and tuning effect, they showed how an idealized model can be used to describe the essential dynamics and performance of absorbers. In another numerical work Sivaprasad et al. [22] developed methods based on inverse sensitivity analysis of damped eigensolutions and frequency response functions and identified system parameters, especially for large-scale vibrating systems. Perlov and Alesov [23] studied transient and steady-state modes of vibration and obtained generalized tensions and displacements of the system as a function of roughness parameters, velocity geometrical, and physical parameters. Besides the hosing system itself, the possibility of the supporting edge damages due to vibration was in the focus of Wang et al. [24] who proposed a relationship with a shear correction factor.

The available literature clearly indicates the significance and necessity of identifying the momentum, thermal and vibration characteristics of fluid transmitting hoses. The focus of the present research is to computationally evaluate and scientifically survey the operational performance of a hose that is in use in the 1.3 SDE 75 CV type FIAT engine. The numerical analyses and investigations performed on the hose are planned and coordinated in accordance with the corresponding FIAT standard [25]. As the findings on momentum and thermal characteristics are interpreted in terms of streamlines, pressure and temperature distributions, and sectional details, the impacts of vibration are demonstrated through in-time variations of overall pressure losses and section-based displacements.

2 Theoretical background

2.1 General remarks

It is stated in the FIAT standard [25] that the air is supplied with a mass flow rate of $\dot{m}$=0.085 kg/s at the hose inlet where the inlet boundary conditions on pressure (gage) and temperature are P_{in}=130 kPa and T_{in}=90°C, respectively. As the ambient condition on temperature is given as T_{amb}=30°C, the primary condition that must be satisfied by the hose is denoted as the pressure loss in the hose with the upper limit of ΔP_K=2 kPa. From this precondition, it can be expected that handling only the momentum transfer mechanism, or the velocity and pressure features, of the air flow would be sufficient to identify the level of pressure loss in the hose. However, as very well known by every related scientist and involved research engineer, one of the main determinative parameters of ΔP_K is the fluid viscosity, which significantly depends on the intensity of flow temperature. Thus, not only

to carry out a realistic and trustable study but also to satisfy the international scientific norms, the energy transfer mechanism, or the temperature variations, must simultaneously be taken under inspection with momentum transfer. The above specifications are generated for the steady flow in the hose. It is obvious that while solving the governing equations on momentum and energy transfer, the key items emerge as computing speed, geometry handling, meshing and post-processing. For these reasons, ANSYS FLUENT v.12.0.1 [26], which is known to be applicable in every major physics discipline with a satisfactory simulation strategy, is run on a AMD Quad Core with 8-GB memory computer in this work.

The main aim of this investigation can be outlined shortly as to evaluate the performance of a recently designed intercooler connection hose, which can also be labeled as of the traditional sort. Since an intercooler connection hose is composed of two parts, the metal and the rubber, from material and manufacturing point of view, distinctions among them, those need to be noticed as important, must be identified and incorporated in the computations accordingly.

2.2 Computational methodology

2.2.1 Analyses on fluid domain

The analyses, in all cases studied in this work, compromised both a utilized a cell-centered formulation with one finite volume per mesh element and pressure-based finite-volume formulations where the methodological integration was carried out by ANSYS FLUENT v.12.0.1 [26]. As the schemes of Rhie and Chow [27] were utilized in the pressure–velocity coupling, a collocated variable arrangement was employed in the simulations. FLUENT was supported by the segregated solution algorithm; moreover, combination of first- and second-order spatial discretisations and second-order transient discretisations were applied in all simulations. The turbulent flow character in the hose is handled by realizable k-ε turbulence model, which is considered to be a sensitive solver-mode for internal flow applications. Besides, as the streamwise density variation of air is integrated into the computations with the ideal gas approach, the precision of the boundary layer calculations are promoted by enhanced wall treatment by adjusting the y^+ value to ~1. Successive computations shown that the notably dense meshing strategy in the vicinity of the hose walls let the turbulence analysis to be carried out with first order upwind approximations; however, momentum and energy transport mechanisms were characterized through second-order upwind approximations. A diffusion transport equation is additionally used to smoothly propagate the motion at boundaries into the solution domain. As the problem considered here involves the vibration of the hose, the requirement on the time-based permanent physical coupling of the fluid and solid domain meshes, on the neighboring surface, arises. Due to this fact, not only to fit the necessities of the engineering scenario but also to promote the computational efficiency and convergence of the overall analyses, the mesh-frame of the fluid domain, adjacent to the solid boundary, is treated as a flexible body moving with it. This conceptual process is carried out through the fluid–solid interaction (FSI) interface of ANSYS, where the basics are expressed in the subsection of 2.2.3. Moreover, the remaining mesh is structured as deformable to absorb the motion using a spring analogy smoothing algorithm.

2.2.2 Analyses on solid domain

A variety of analyses types, such as static, transient, harmonic, etc., and a broad range of single and coupled field element types are supported and can be integrated by the ANSYS v.12.0.1 finite element analysis code. The hose is modeled in thin shell form, where the investigations used only flexible dynamic (i.e., transient) analysis with linear structural elements. Moreover, the complete set of simulations was based on the time integration method proposed by Chung and Hulbert [28].

2.2.3 Analyses on FSI

In this phase of the analyses, the scientific requirement is to strongly achieve the coupled solution of the fluid–structure interaction problem. To satisfy this need and to couple the fluid and structural solution fields for the flow-through vibrating hose simulations, a partitioned approach with stagger (or coupling) iterations, namely the MFX variant of the ANSYS MultifieldTM solver, was used. In the solution procedure, each time step is broken into a sequence of stagger iterations by the partitioned approach. Within each individual stagger iteration step (1) to satisfy all types of convergence criteria in the fluid and structural field equations, stagger iterations are executed, (2) the load vectors are evaluated, (3) the fluid problem is solved by the transfer of the displacement load vectors from the ANSYS to the FLUENT solver, and (4) the structural problem is solved by the transfer of the force load vectors from the FLUENT to the ANSYS solver.

2.3 Boundary conditions

While performing a numerical investigation for an intercooler connection hose, three issues will be significant due to the fact that the hose is designed to operate in a predefined engine. Two of these issues can be grouped

within the boundary condition set; explicitly, they are the turbulence level (Tu) of the air at the hose inlet and free convection behavior around the exterior border of the hose lateral surface. On the other hand, the third issue regards the certain portion of the hose: namely the rubber part. Since the cooled air, downstream of the charged air cooler (CAC), is expected to enter the hose, the heat exchanger function of the CAC will also raise the turbulence intensity. For this reason, at the hose inlet the turbulence level is assigned the value of 2%, which will be helpful as well to monitor the upper limit of the pressure loss in the hose. Indeed, with the emergence of the Reynolds number at the hose inlet as $Re_{in} \approx 50 \times 10^3$ during the computations, also promoted the choice on turbulence level to a more trustable appearance. The second issue is the free convection coefficient (h) around the hose. To evaluate this value, the widely accepted scientific formula of Eq. 1a [29] is employed, with the Nusselt and Grashof number definitions of Eq. 1b and Eq. 1c, respectively.

$$Nu = \left\{ 0.60 + \frac{0.387 \times (Gr \times Pr)^{\frac{1}{6}}}{\left[1 + (0.559/Pr)^{9/16}\right]^{8/27}} \right\}^2 \tag{1}$$

$$Nu = \frac{h \times d}{k_f} \qquad Gr = \frac{g \times \beta \times (T_s - T_{amb}) \times d^3}{\nu^2}$$

The data for the fluid properties of thermal expansion coefficient (β), Prandtl number (Pr), conduction coefficient (k_f), and kinematic viscosity (ν) are obtained from Ref. [29] at the film temperature of T_f=60°C=333.15 K (=(T_s+T_{amb})/2) as $\beta = 1/T_f = 1/333.15 = 3.0017 \times 10^{-3}$ 1/K, Pr=0.70236, $k_f = 2.8753 \times 10^{-2}$ W/mK, and $\nu = 1.923 \times 10^{-5}$ m^2/s, respectively. From these values, Grashof and Nusselt numbers appear as Gr=435,378 and Nu=10.464. Lastly, the free convection coefficient is calculated as h=6.7 W/m^{2}K. For the rubber part, the density (ρ), conductivity (k), and specific heat (C) are taken as ρ=905 kg/m^3, k=0.12 W/mK, C=1,925 J/kgK [30, 31]. Moreover, the surface roughness of the rubber part is taken as ε=32 μm (in RMS) that can be accepted as the upper limit.

On the other hand, the input strategy in the computational analyses must not only fit the engineering requirements of the hose function in the engine but also be compatible with the related treatments of ANSYS's algorithmic logic. In the flow and heat transfer investigation section of the research, the mass flow rate ($\dot{m}$=0.085 kg/s) and air temperature (T_{in}=90°C) are defined at the hose entry as inlet boundary conditions. At the hose outlet, the exit boundary condition is employed in terms of gage pressure (P_{ex}). A series of computations are carried out with different exit pressure conditions; the P_{ex} that results in the hose entry value of P_{in}=130 kPa resolves the operational frame. For the vibrating hose analyses, as the intercooler connection plane of the hose is kept stationary, the engine side is excited with simple harmonic motion $\left(\eta(t) = \frac{H}{2}\sin\left(\pi \frac{t}{T}\right)\right)$, having the wave height and period values of H=2 mm and T=0.01 s, respectively.

Since the overall error in the computations is mainly a combination of grid density and iteration number (or convergence criterion), several successive runs are performed to ensure that the numerical outputs are free of the roles of computational items. Tables 1 and 2 display a summary of these tests both for the fluid and solid domains in terms of the fluid flow and heat transfer parameters and vibration displacements that are the primary concerns of the present research. For the complete set of scenarios investigated, a convergence criterion of 1×10^{-7} is used to certain negligibly small iteration errors. Both the employed mesh and the applied converge criterion guarantee as well the reliable stance and the validity of the evaluated outputs.

In the 1st step of our project, we analyzed the flow and heat transfer characteristics of air in the hose, by fixing the hose to stationary position. In this step, we aimed to compare the compatibility of the pressure loss value of the metal hose with the FIAT standard [25], which will also serve as a guide from the point of meshing strategy of the flow path. In the 2nd step, we employed a simple harmonic motion to the engine side of the hose to demonstrate the influence of vibration on the operational characteristics of the subject hose.

3 Results and discussion

Figure 1 displays the general scene of the intercooler connection hose. It can be seen from the figure that the intercooler connection is the rubber part that is shown on the left hand side of the view; whereas, the exit section of air is on the metal part of the hose. In the manufacturer's catalog [32], the FEP04 type steel with code: 6114 is denoted as a low carbon kind, thus the necessary data for the steel part are gathered as ρ=8,131 kg/m^3, k=41.8 W/mK, C=499 J/kg K [29, 32]. Besides, the roughness of the

Table 1 Grid node effects on fluid flow and heat transfer parameters (fluid domain)

# of nodes	ΔT (°C)	ΔP_k (Pa)	$\dot{m}$ kg/s
652,748	0.89	1.83	0.091
739,451	0.85	1.67	0.088
881,784	0.82	1.56	0.086
1,026,543	080	1.51	0.085
1,105,140[a]	0.80	1.50	0.085

[a] Optimum grid nodes

Table 2 Grid node effects on fluid flow, and vibration displacements (solid domain)

# of nodes	ΔP_k (Pa)		Displacement (mm) (plane 1)	
	t=0.01 s	t=0.04 s	t=0.01 s	t=0.04 s
6,749	1.79	1.72	4.77	10.31
7,823	1.71	1.67	4.63	10.27
8,673	1.59	1.58	4.57	10.06
9,327	1.56	1.51	4.46	9.98
9,514[a]	1.56	1.51	4.45	9.96

[a] Optimum grid nodes

metal part is also very important from the point of pressure losses. Industrial and scientific knowledge [33] indicates that a roughness of ε=3.2 μm is a frequent and realistic value for practical steel applications including deep drawing [34].

3.1 Stationary case analysis

3.1.1 Overall characteristics

Computational fluid dynamics (CFD) analyses are carried out with ANSYS FLUENT v.12.0.1. It is well known in CFD study that the employed mesh in the considered fluid and solid regions is vital from the point of not only accuracy and convergence of the computations but also the run times. Thus, to determine the optimum meshing strategy, successive computations are performed with the identical boundary conditions but with different mesh densities. Figure 2 displays the best possible adaptation, where the fluid domain is meshed with a number of 1,105,140 elements. Analyses are performed with the boundary conditions stated in the previous sections of this paper. The main input variables can once more be stated here as the inlet gage pressure (P_{in}=130 kPa) and temperature (T_{in}=90°C), the mass flow rate ($\dot{m}$=0.085 kg/s), and the ambient temperature (T_{amb}=30°C). In addition to the boundary conditions, the allowed pressure loss is indicated as ΔP_K=2 kPa. Computations on the momentum and heat transfer mechanisms generated complete pressure, velocity and temperature distribution layouts in the air domain of the hose. To check the compatibility of the employed numerical algorithm with the flow characteristics, the fundamental fluid mechanics definition of Reynolds number is computed at the hose inlet. The outcome of $Re_{in}\approx 50\times 10^3$ not only points out turbulent flow character in the hose but also verifies the implemented computational methodology.

Since the major concern of hose design is to limit the amount of pressure loss below 2 kPa, being the primary output of the executed study, the gage pressure at the hose exit must be given at the first hand. The exit pressure and the corresponding pressure loss in the hose are determined as P_{ex}=128.50 kPa and ΔP_K=1.50 kPa, where these numbers clearly put forward that the hose satisfies the related FIAT documentation/standard. Moreover, another important issue in the air flow is the variation of temperature level. Computations shows that under free convection boundary condition, the heat transfer from the hose walls causes an inconsiderable decrease of flow temperature; such that the exit temperature and temperature decrease of air come out to be T_{ex}=89.20°C and ΔT=0.80°C.

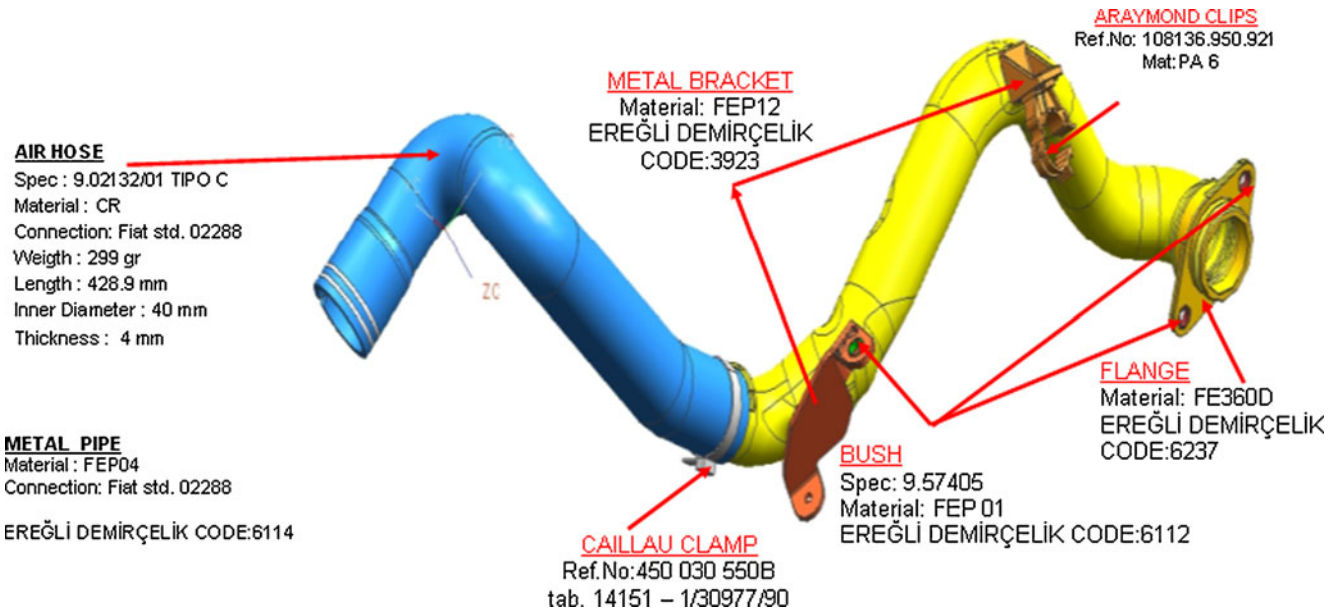

Fig. 1 General scene of the hose

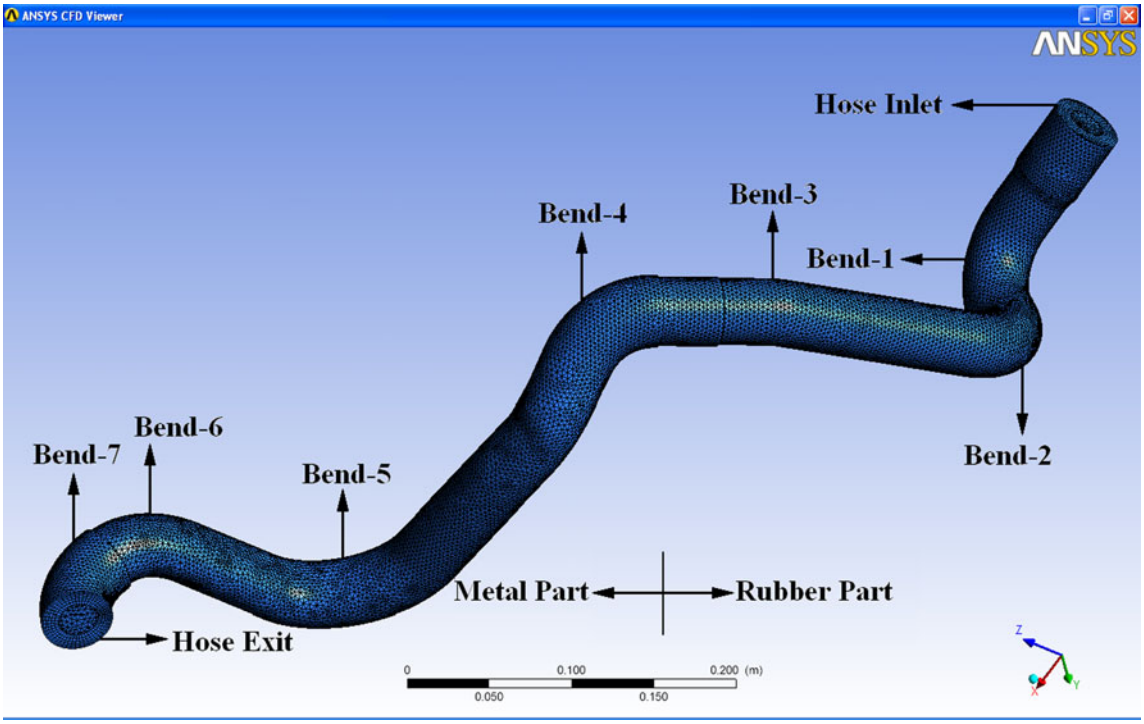

Fig. 2 Meshed hose with specific locations

Although these outputs are sufficient to justify the design appropriateness of the subject hose, the computations additionally point out that the property variations in the hose are non-linear and exhibit local peaks and dips. These local maxima and minima are most recognizable downstream of the "*Bends*" that are marked in Fig. 2. Indeed, from scientific point of view these non-linearities are expected consequences of non-straight flow passages and they attract the attention of every related researcher due to their direct contribution on the energy loss and power transmission of the complete engineering assembly.

The pressure distribution on the interior surface of the hose is given in Fig. 3. As the legend displays, the maximum pressure inside the hose exceeds the inlet value of 130 kPa and the minimum one is lower than the exit pressure (128.50 kPa). This outcome can be detailed through the interactions of pressure and velocity terms in the momentum transfer mechanism of the flowing air. The bends, while guiding the flow to follow the desired path between the inlet and exit sections of the hose, not only cause the air velocity to vary both in direction and magnitude but also manipulate the measure of pressure. For this reason, the velocity characteristics inside the hose express a significant impact on the pressure map, therefore on the overall pressure loss in the hose.

Figure 4 presents the overall flow behavior of air in terms of streamlines. To provide a more detailed visual inspection opportunity, the flow domains are zoomed around Bends 1 and 2 and 6 and 7 and displayed in Fig. 5. The focused views apparently identify the flow swirl, where this structure is commonly referred to as rotational flow. Scientific investigations on this branch of discipline determined and proved that such interactions have strong impacts on both pressure and temperature, resulting in stronger deviations in either.

To validate the statements on the role of flow activity on the energy transfer mechanism, the overall temperature characteristics in the hose is given in Fig. 6. The regional differences and neighboring shifts are evident and recognizable. The panoramic view of the overall characteristics given here clearly shows that the hose geometry, including the straight sections and bends, is dominantly determinative on the local behavior of the flowing air and the so occurring momentum and heat transfer interactions with the hose walls. Therefore, from a scientific and industrial perspective, sectional details of the pressure, velocity, and temperature must also be identified to categorize the sources of local and overall variations of pressure and temperature.

3.1.2 Sectional details

As defined in the previous part of this report, due to the non-linear variation behaviors of the pressure, velocity, and temperature of flowing air, these data may attain maximum and minimum levels at certain locations in the hose. For this reason, it is aimed to focus especially on the "*Bends*" that are specified in Fig. 2. Table 3 displays the local data,

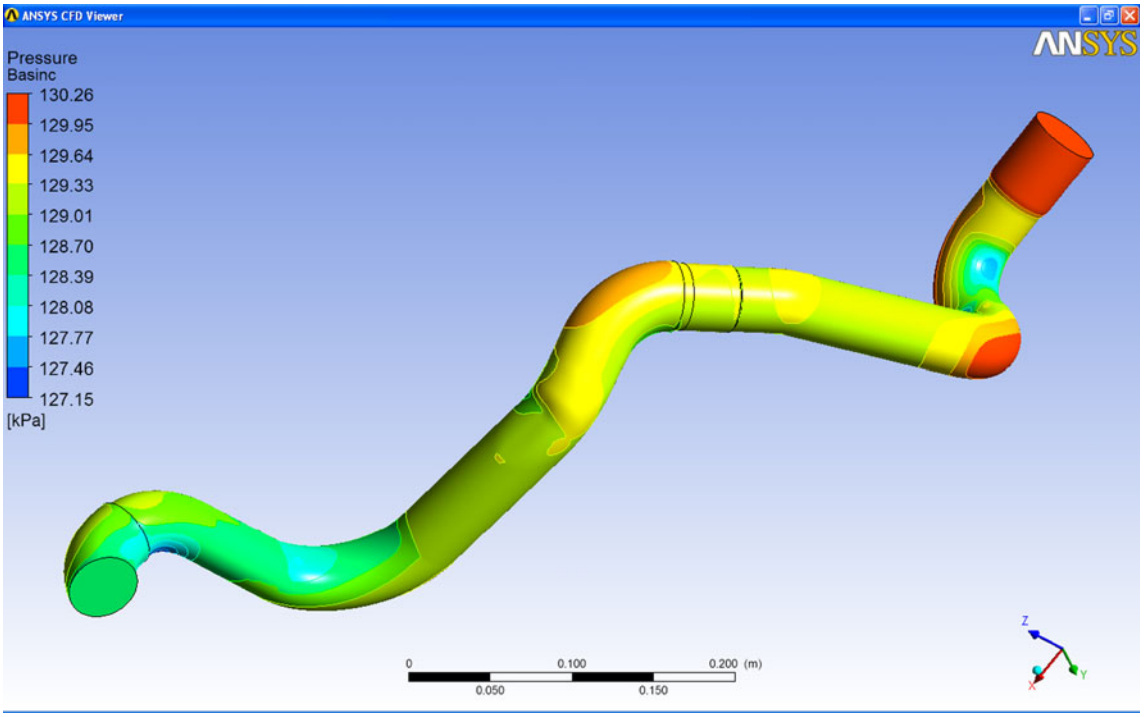

Fig. 3 Overall pressure characteristics

evaluated at the inlet and exit sections of the 7 bends (Fig. 2), together with the deviations among the boundaries of these bends.

It can be inspected from the table that pressure values neither continuously decrease in the flow direction nor decrease with a unique trend. Moreover, at Bends 4 and 7 flow pressure is computed to rise by 0.07 and 0.26 kPa, respectively. It can scientifically be declared that, to provide a deeper insight on the mechanism, the three data sets for pressure, velocity, and temperature must be discussed in

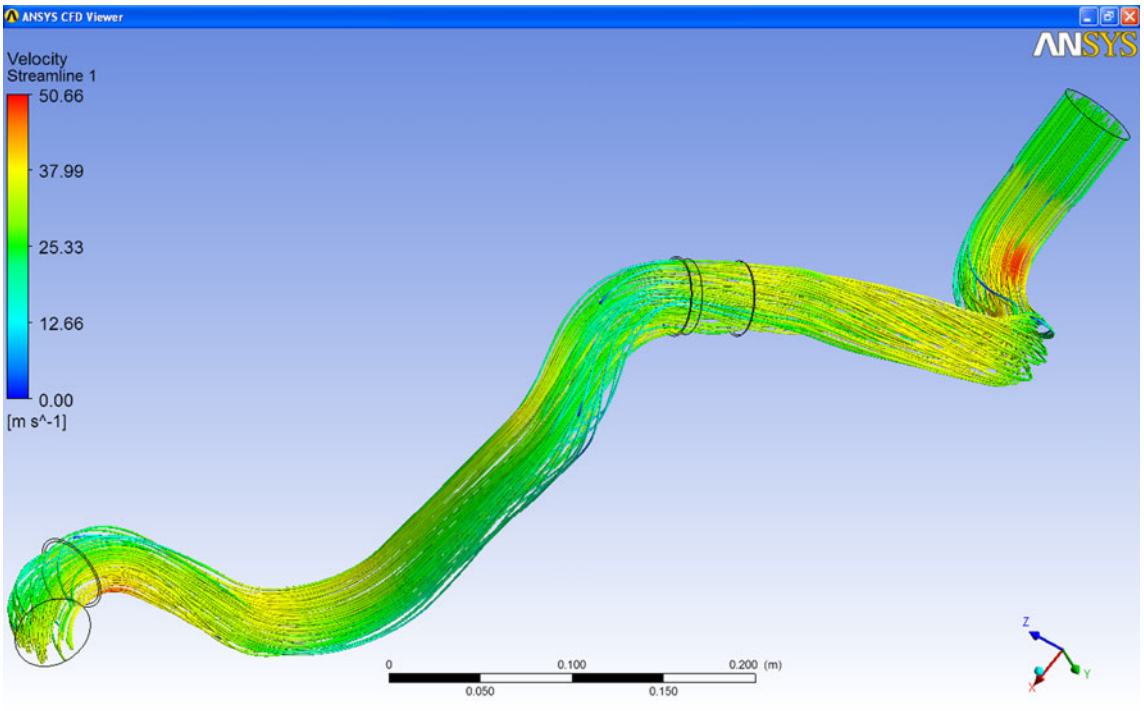

Fig. 4 Overall velocity characteristics

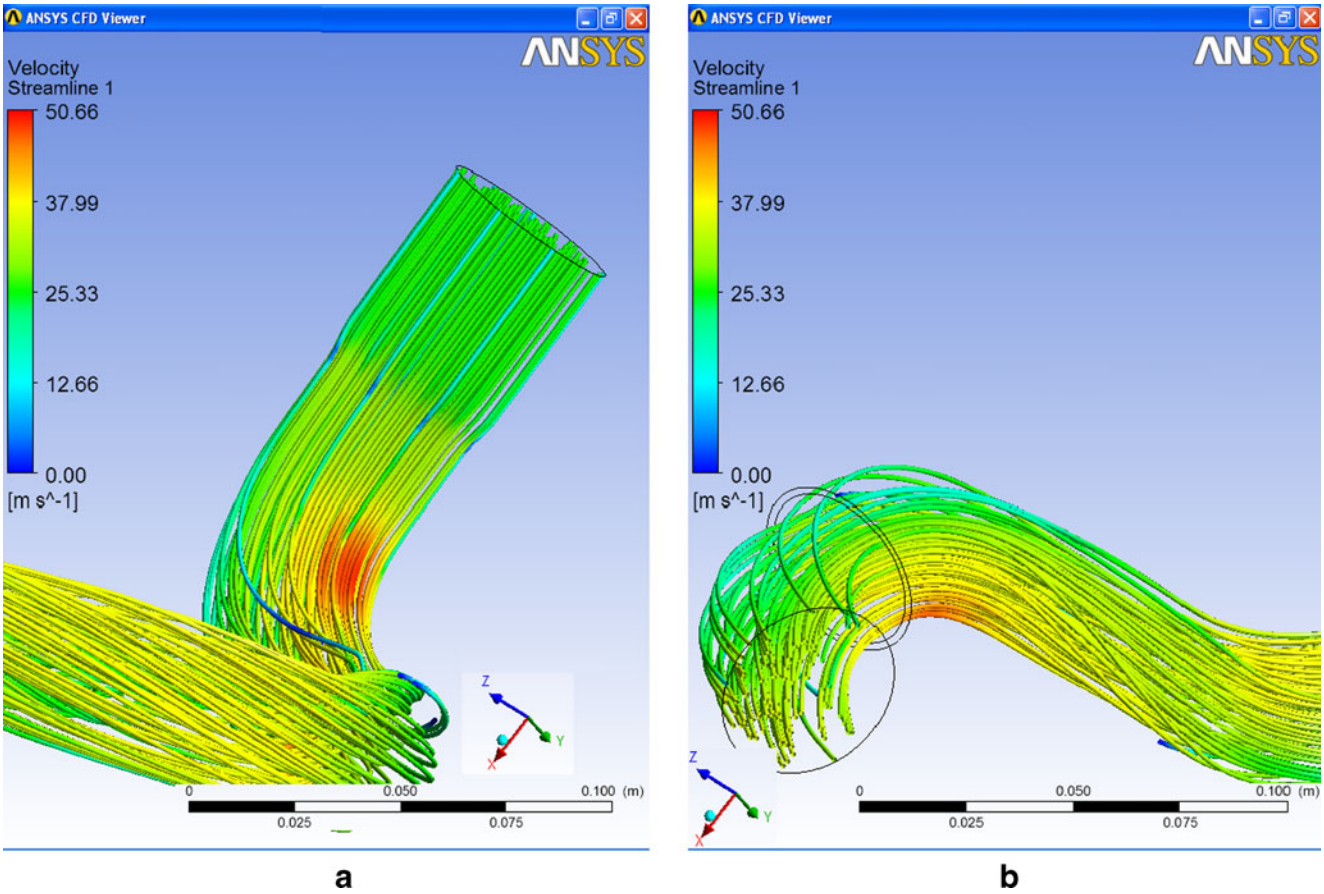

Fig. 5 Velocity characteristics around bends **a** 1 and 2 and **b** 6 and 7

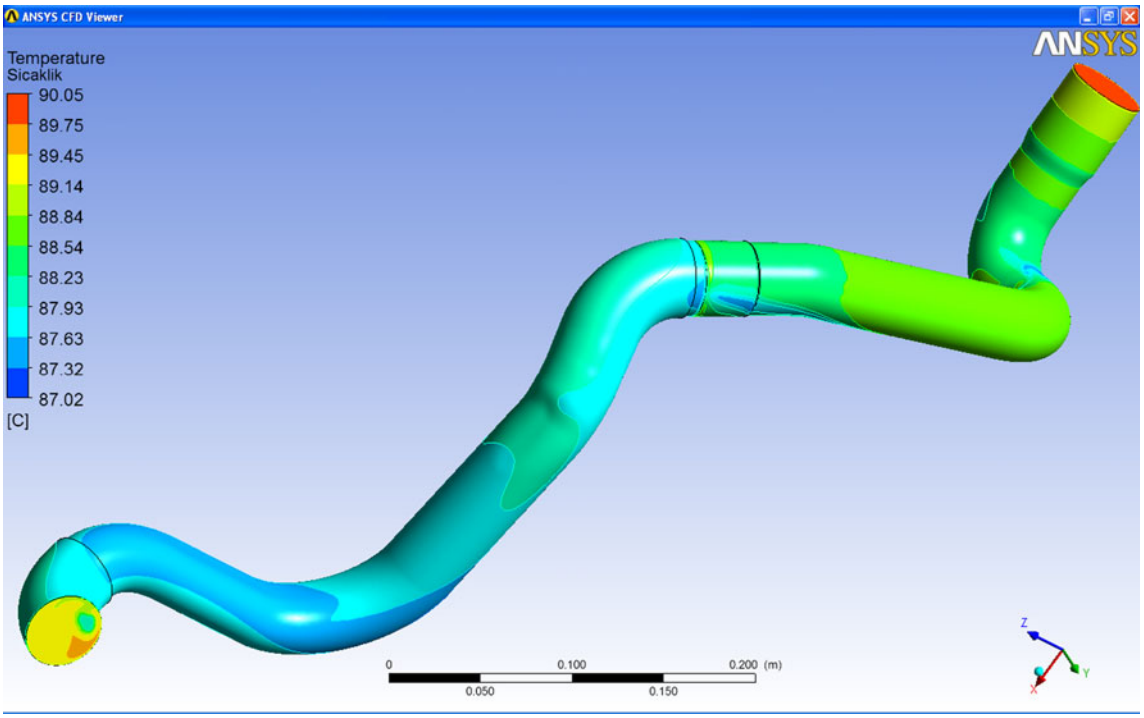

Fig. 6 Overall temperature characteristics

Table 3 Flow and thermal data at the specific sections of the hose

	Bend number	Inlet/exit section	Average pressure (P; kPa)	Average temperature (T; °C)	Average velocity (V; m/s)	ΔP_k ($P_{in}-P_{ex}$; kPa)	ΔT ($T_{in}-T_{ex}$; °C)	ΔV ($V_{ex}-V_{in}$; m/s)	V_{mean} (m/s)
Hose inlet			130.00	90.00	25.81				
	1	Inlet	129.59	89.78	30.96	0.27	0.11	0.29	31.11
		Exit	129.32	89.67	31.25				
	2	Inlet	129.32	89.67	31.25	0.04	−0.01	0.56	31.53
		Exit	129.27	89.68	31.81				
	3	Inlet	129.17	89.66	31.34	0.03	0.01	0.18	31.43
		Exit	129.15	89.65	31.52				
	4	Inlet	129.26	89.65	26.92	−0.07	−0.07	−0.66	26.59
		Exit	129.33	89.72	26.26				
	5	Inlet	129.12	89.56	26.96	0.39	0.19	5.26	29.59
		Exit	128.73	89.37	32.22				
	6	Inlet	128.62	89.30	32.24	0.03	0.02	−0.38	32.05
		Exit	128.59	89.28	31.86				
	7	Inlet	128.59	89.28	31.86	−0.26	−0.16	−5.44	29.14
		Exit	128.44	89.44	26.42				
Hose exit			128.20	89.20	27.28				

conjunction. The *Bend-Based* data clearly put forward that both the pressure and temperature variations in the hose are significantly characterized by the velocity values/variations. Whether the velocity values are increasing or decreasing and also the magnitude of these variations, the mean velocity, the cross-sectional area of the hose and its narrowing/diverging design and the vortex structure, in terms of domain extend and strength, come out to be the fundamental factors on the pressure and temperature features of hose flow.

To identify the interrelation of momentum and thermal characteristics of the air flow in the hose, the cross-sectional distributions of velocity (Fig. 7), pressure (Fig. 8), and temperature (Fig. 9) are displayed at the inlet and exit sections of Bend 7 (Fig. 2). It can be visualized from Fig. 7a that towards the hose exit the flow domain is significantly distorted due to the previous six bends in the flow direction. The very thin no-slip region, neighboring the solid wall, is followed by the fluid structure that is mainly influenced by the downstream action of Bend 6, together with the centrifugal forces acting within Bend 7. Towards the exterior curve of Bend 7, flow experiences serious accelerations such that the velocity levels rise up to U=46.56 and U=45.1 m/s at the inlet and exit sections (Figs. 7a, b), where the average values are U=31.86 and U=26.42 m/s (Table 3). The downstream action of Bend 6 is most recognizable at the inlet section of Bend 7, developing the secondary vortex system where the local velocity significant decreases (Fig. 7a).

Within Bend 7, the velocity vectors are directed towards the exterior curve of the bend (Fig. 5b) which as a consequence cause the collision of the fluid particles with those solid regions. Since the magnitude of these collisions varies locally, the resultant pressure distribution becomes self defined (Fig. 8a). Such that, in spite of the overall pressure loss amount in the flow region between the Hose Inlet and Bend 7, the pressure data locally exceeds the inlet value with 130.06 kPa. On the other hand, the manipulated momentum activity at the exit section not only develops a distinct pressure pattern but also shifts the domains of minimum and maximum pressure (Fig. 8b). Indeed this outcome can also be seen from the overall pressure characteristics of Fig. 3.

Figure 9 demonstrates similar structures in temperature distributions with that of pressure from the point of momentum impact. In both inlet and exit sections of Bend 7, evident deviations in the temperature distributions are present, where the sources of these deviations are different. As the thermal deformations at the inlet section (Fig. 9a) are due to the upstream characteristics of Bend 7, including the comparably lower values within the sub-vortex domain of Fig. 9a, the exit section values (Fig. 9b) are mostly characterized by the centrifugal impacts.

The discussions carried out here, on both the streamwise handling of flow route data (Table 3) and velocity, pressure and temperature distributions of a specific flow-section (Figs. 7–9) in the hose, clarified that although the main aim in the design methodology of engine hoses is to satisfy the related standard which can just be confirmed through the inlet and exit plane values, the sub-design issues and steps must also cover detailed investigations on the local and sectional aspects. For these reasons, we very strictly believe and affirm the necessity of detailed CFD analyses to create the technical ground to propose and develop more efficient and functional hose designs.

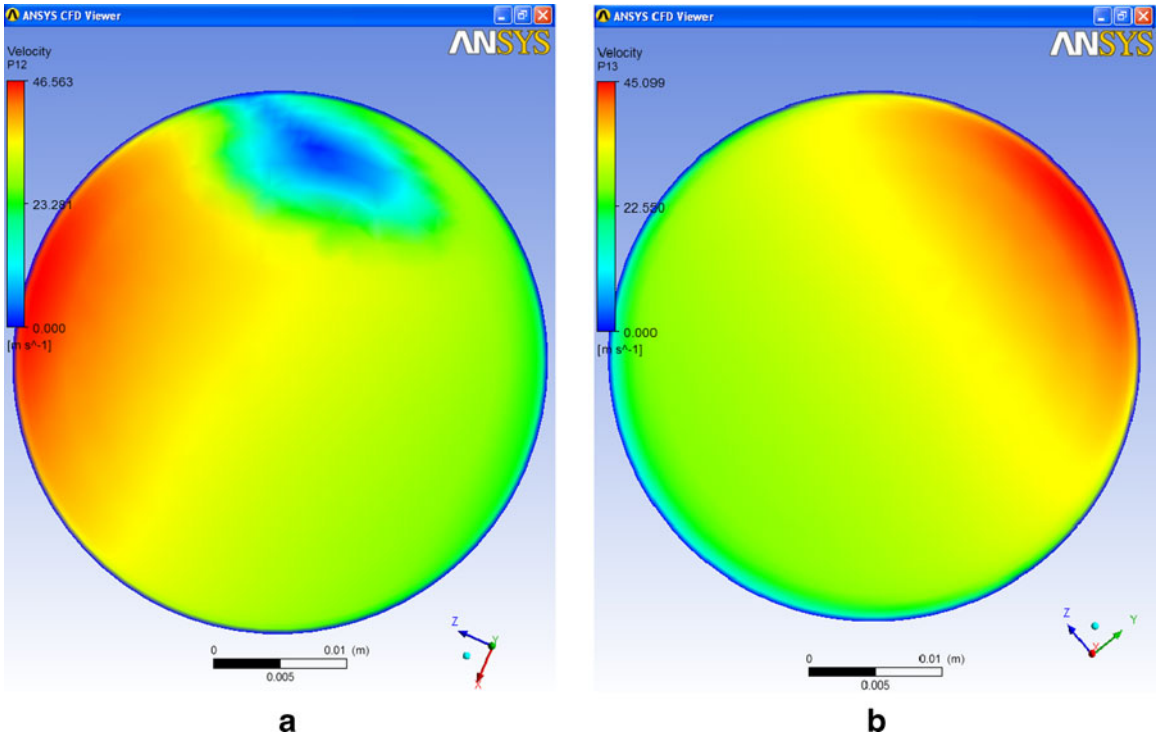

Fig. 7 Velocity distributions at the **a** inlet and **b** exit sections of Bend-7

3.2 Vibrating case analysis

The present phase of the research is aimed to investigate the impact of vibration on the momentum—thermal characteristics of air flow in the intercooler connection hose. Since the implementation of vibration to the hose will result in elastic deformations, to carry out the FSI methodology efficiently, the necessary modulus of

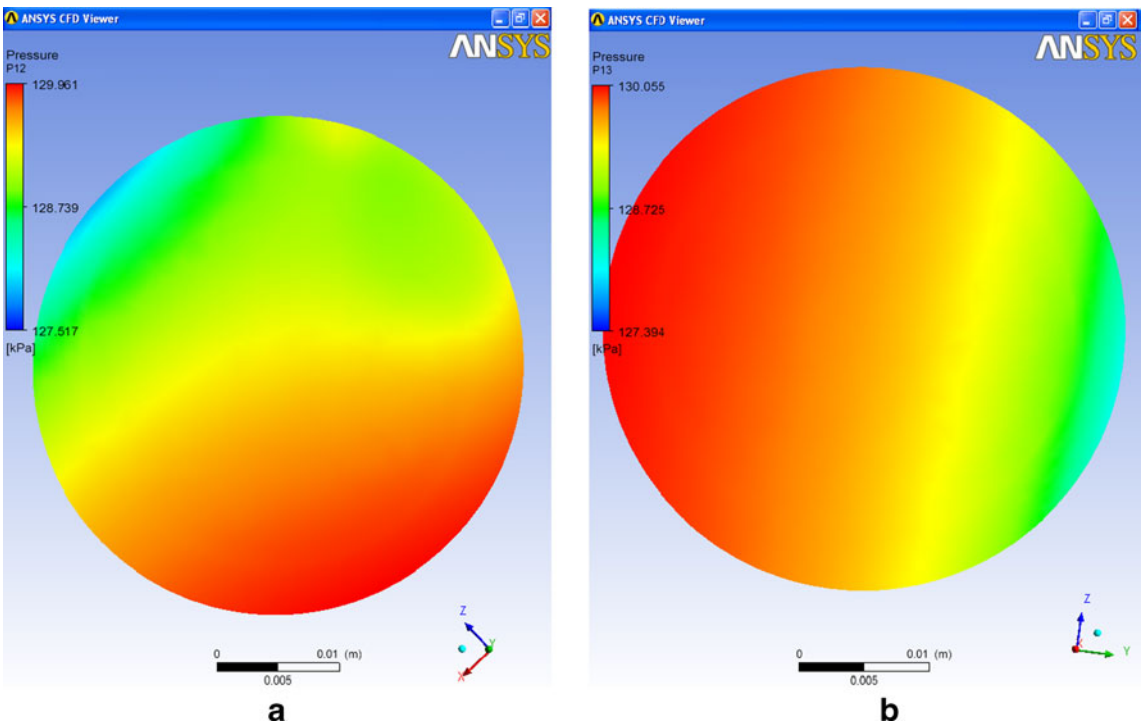

Fig. 8 Pressure distributions at the **a** inlet and **b** exit sections of Bend-7

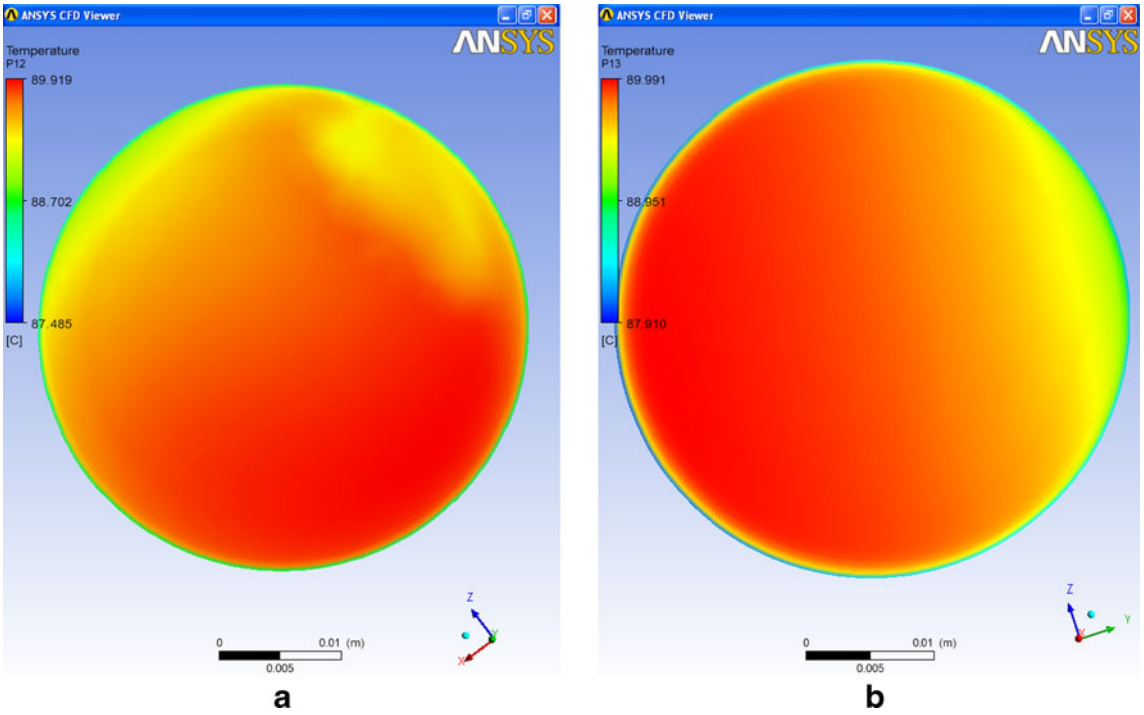

Fig. 9 Temperature distributions at the **a** inlet and **b** exit sections of Bend-7

elasticity data for the steel and sections are selected as E_{steel}=200 GPa and E_{rubber}=10 MPa, respectively.

To characterize the role of vibration not only on the hose body but also on the flowing air inside the hose, two-way FSI procedure is used in the analysis. In spite of the extensive research that has been carried on the operation characteristics of internal combustion engines, the available literature is incapable of providing a real time data on engine vibration. Thus, the vibration mechanism is implemented into the operation in the form of simple harmonic motion (SHM). As the engine side of the hose is excited with a wave height and period of H=2 mm and T=0.01 s, respectively, the intercooler connection plane is kept stationary. The open form of the employed vibration displacement is $\eta(t) = \frac{H}{2}\sin\left(\pi\frac{t}{T}\right)$. Analysis shows that due to the presence of the applied vibration on the engine side, the pressure loss values in the hose vary in time. Computations resulted in a pressure loss range of ΔP_{K}=1.35–1.76 kPa (Fig. 10) in the time domain of t=0–0.05 s, which corresponds to five cycles. Figure 10 points out that the in-time variation of the ΔP_{K} values are not symmetrically repeating. This evaluation can be attributed to the significantly distinct elasticity modulus values of steel and rubber, causing not only random structural oscillations but also so-generated FSI activity. Computations additionally indicated that the pressure values in the hose vary in the range of P_{s}=127.03–130.73 kPa, where the local pressure values are neither stable as well.

Vibration of the engine hose is not only important from the point of the FSI mechanism and the so-elevated pressure loss values but also due to the possibility that the vibrating hose can physically get in touch with the surrounding components of the engine. For this reason, the in-time variation of the vibration displacements of the various sections of the hose may gain additional significance. Figure 11b displays the vibration characteristics of the five sections that are indicated in Fig. 11a. The metal section of the hose comes out to behave comparably rigidly with respect to the rubber part (Fig. 11b), such that the maximum displacement of the rubber part is almost threefold of the corresponding steel section value. Simulations additionally indicated that the oscillations of the steel and rubber parts have independent frequencies, where the extremums appear at different instants in time. The characterizing issues can be identified as the application location of the SHM and the differences in the lengths and the elasticity modulus values of the two hose parts.

4 Conclusions

In this research, computations are performed with ANSYS FLUENT v.12.0.1 and the analyses are based on the inlet and boundary conditions that are defined in the related FIAT documentation/standard. Since the main operational expectation from the hose is to transport the air between the

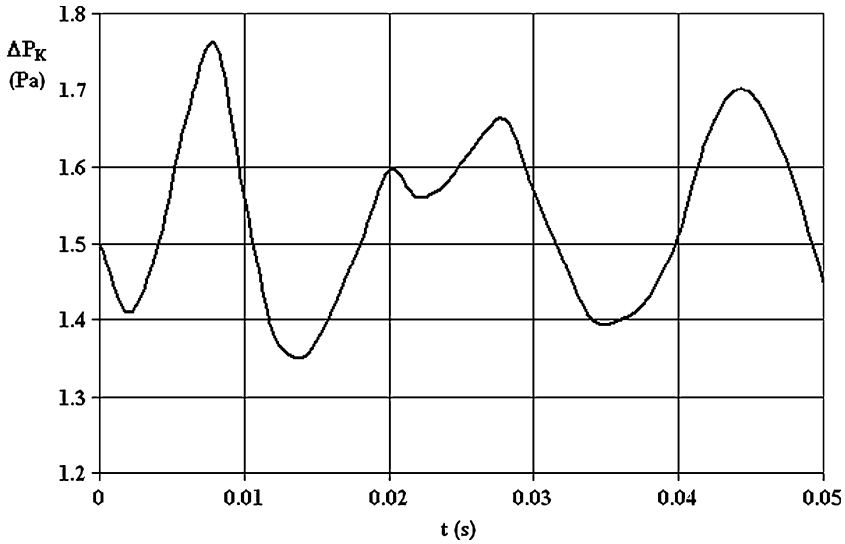

Fig. 10 In time variation of pressure loss

CAC and the engine with less than 2 kPa of pressure loss, it can explicitly be stated that the hose is capable of delivering the air with a pressure loss value of ΔP_K=1.50 kPa, which is below the acceptable upper pressure loss limit. However, handling the computational outputs with a technically deeper vision and with an academically experienced talent also points out the necessity of configuring the design process and methodology by assembling the complete set of

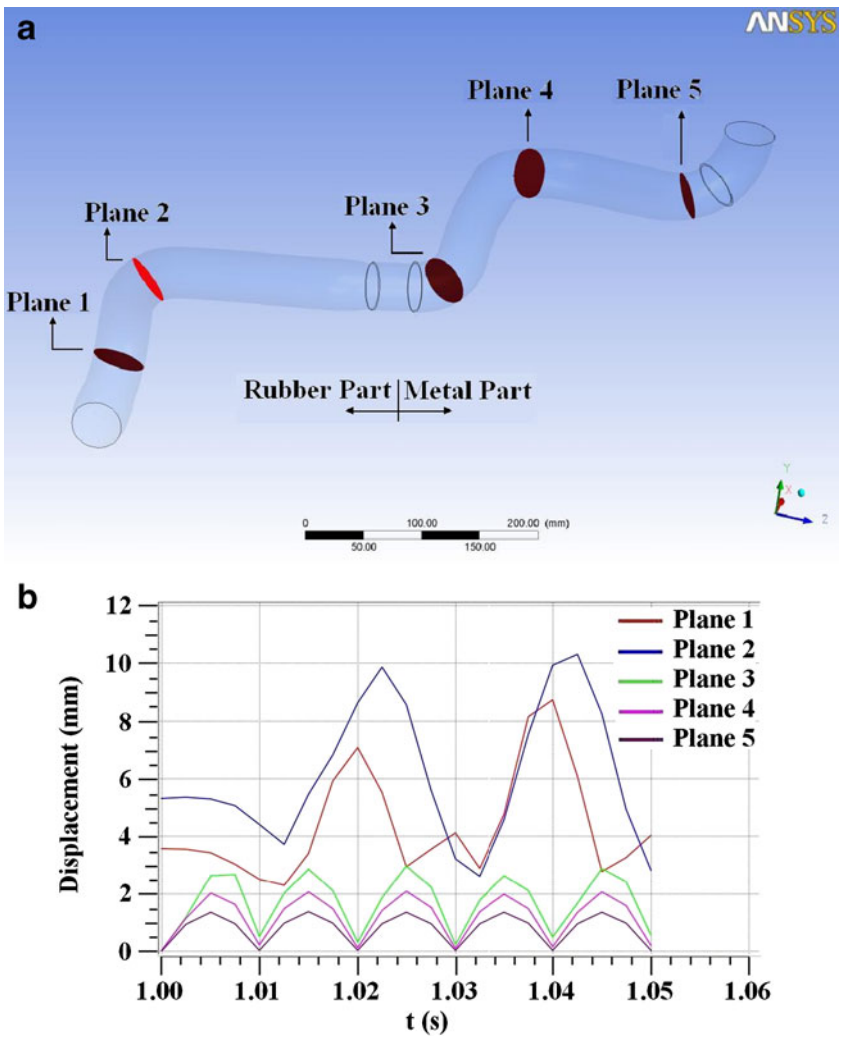

Fig. 11 **a** Investigated locations for vibration mechanism. **b** Vibration displacements

parameters that have influence on the overall performance of the intercooler connection hoses. On the other hand, in the presence of vibration, computations resulted in a pressure loss range of ΔP_K=1.35–1.76 kPa. Numerical analyses additionally have shown that, the impact of vibration generates diverse fluctuation schemes at different sections of the hose, where the influential issues can be stated as the application location of the SHM and the different length and elasticity modulus values of the two hose parts. Moreover, the steel and rubber parts are determined to oscillate with independent frequencies, such that the extremums appear at different instants in time. The main deductions on the performance scheme of the intercooler connection hose can be itemized as follows:

- The intensity of the pressure loss is compatible with the corresponding FIAT standard, indicating the design success of the hose from the operational point of view.
- The diameter of the hose not only fits the overall structural layout of the engine but also generates acceptable flow velocities that are quite determinative on the pressure loss levels.
- In addition to directing the flow in the appropriate route in between the engine components, the bends in the geometric design of the hose are as well capable of not resulting in excess pressure losses.
- The metal part of the hose suppresses the vibration induced displacement values; however increases the total mass of the hose.
- By simultaneously considering the pressure loss, total mass and displacement characteristics, the lengths and the percent based existence of the metal and rubber parts can be reoriented, which in return will improve the overall design success of the intercooler connection hose.

Nomenclature

C	Specific heat (J/kg K)
d	Diameter (m)
g	Gravitational acceleration (m/s^2)
Gr	Grasshof number
h	Convection coefficient (W/m^{2}K)
H	Vibration amplitude (m)
k	Conduction coefficient of solid (W/mK)
k_f	Conduction coefficient of air (W/mK)
$\dot{m}$	Mass flow rate (kg/s)
Nu	Nusselt number
P	Pressure (Pa)
Pr	Prandtl number
Re	Reynolds number
t	Time (s)
T	Temperature (K) and vibration period (s)
U	Air velocity (m/s)
ΔP_K	Pressure loss (Pa)
ΔT	Temperature drop (K)

Greek symbols

β	Thermal expansion coefficient (1/K)
ε	Surface roughness (mm)
η	Vibration displacement (m)
ν	Kinematic viscosity (m^2/s)
ρ	Density (kg/m^3)

Subscripts

amb	Ambient
ex	Exit
in	Inlet
s	Surface, Static

References

1. Schroden T, Keuper D (1991) Development of a high-tech hose for a high-tech car turbo engine. Kautsch Gummi Kunstst 44:872–878
2. Maihle FL (1986) Safety concerns on hose and engine pressures. Fire Eng 139:16–16
3. Baaser H (2007) Global optimization of length and macro-micro transition of fabric-reinforced elastomers with application to a brake hose. Comput Mater Sci 39:113–116
4. Cooke R, House R, Lawson IJ (2001) Hand-arm vibration syndrome from exposure to high-pressure hoses. Occup Med-Oxford 51:401–409
5. Kain RM (2000) Case history—ambient temperature SCC of stainless steel high-pressure hose connectors. Mater Perform 39:96–98
6. Hau LN, Wang BJ (2007) On MHD waves, fire-hose and mirror instabilities in anisotropic plasmas. Nonlinear Process Geophys 14:557–568
7. Friedrichs O, Borschulte A, Zuttel A (2008) Controlled mechanically activated hydrogen sorption. Int J Hydrog Energy 33:5606–5610
8. Ilardo R, Williams CB (2010) Design and manufacture of a Formula SAE intake system using fused deposition modeling and fiber-reinforced composite materials. Rapid Prototyp J 16:174–179
9. Ilgamov MA, Ratrout RA (1999) Large deflection of superconducting cable. Int J Non-Linear Mech 34:869–880
10. Cronin K, Byrne E, Leary PO (2007) Prevention of thermo-hydraulic rupture of solvent transfer pipes in the pharmaceutical industry. J Loss Prev Process Ind 20:7–14
11. Rath C, Farjas J, Roura P (2004) Gas renewal in the horizontal furnace of a thermobalance. Thermochim ACTA 412:113–119
12. Cho JR, Song JI, Choi JH (2006) Prediction of effective mechanical properties of reinforced braid by 3-D finite element analysis. Fract Strength Solids 306:799–804
13. Simmons D (1997) High performance environments: the case for polymeric flexible hoses. Polym Polym Compos 5:563–571
14. Stoeckel D, Borden T (1992) Actuation and fastening with shape memory alloys in the automotive industry. Metall 46:668–672
15. Marquez A, Fazzini PG, Otegui JL (2009) Failure analysis of flexible metal hose at compressor discharge. Eng Fail Anal 16:1912–1921

16. Liu YC, Hwang YF, Huang JH (2009) Modes of wave propagation and dispersion relations in a cylindrical shell. J Vib Acoust-Trans ASME 131: article number: 041011
17. Drew JE, Longmore DK, Johnston DN (1997) Measurement of the longitudinal transmission characteristics of fluid-filled hoses. Proc Inst Mech Eng Part I-J Syst Control Eng 211:219–228
18. Nishimura S, Matsunaga T (2000) Analysis of response lag in hydraulic power steering system. JSAE Rev 21:41–46
19. Yu JH, Kojima E (1998) Wave propagation in fluids contained in finite-length anisotropic viscoelastic pipes. J Acoust Soc Am 104:3227–3235
20. Drexel MV, Ginsberg JH (2001) Modal overlap and dissipation effects of a cantilever beam with multiple attached oscillators. J Vib Acoust-Trans ASME 123:181–187
21. Shaw SW, Pierre C (2006) The dynamic response of tuned impact absorbers for rotating flexible structures. J Comput Nonlinear Dyn 1:13–24
22. Sivaprasad R, Venkatesha S, Manohar CS (2009) Identification of dynamical systems with fractional derivative damping models using inverse sensitivity analysis. CMC-Comput Mater & Contin 9:179–207
23. Perlov BM, Alesov MB (1996) Mathematical modeling of spatial vibrations of lengthy hose structures. Ocean Eng 23:257–269
24. Wang CM, Kitipornchai S, Reddy JN (2000) Relationship between vibration frequencies of Reddy and Kirchhoff polygonal plates with simply supported edges. J Vib Acoust-Trans ASME 122:77–81
25. Anonymous (2008) Subsystem functional description (SSFD) for charge air hoses Fiat 225 Euro 5
26. Anonymous (2009) ANSYS FLUENT v.12.0.1 Manual
27. Rhie CM, Chow WL (1982) A numerical study of the turbulent flow past an isolated airfoil with trailing edge separation. AIAA Paper 82-0988
28. Chung J, Hulbert GM (1993) A time integration algorithm for structural dynamics with improved numerical dissipation: the generalized-method. J Appl Mech 60:371–379
29. Incropera FP, DeWitt DP (2001) Fundamentals of heat and mass transfer. Wiley, New York
30. http://www.matsceng.ohio-state.edu/mse205/lectures/chapter20/chap20.pdf. Accessed 25 November 2009
31. http://www.faqs.org/patents/app/20090004416. Accessed 22 November 2009
32. http://www.erdemir.com.tr/images/urun_hizmetler/Katalog_2007_TR.pdf. Accessed 21 November 2009
33. Hocheng H, Pa PS (2003) Continuous secondary ultrasonic electropolishing of an SKD61 cylindrical part. Int J Adv Manuf Technol 21:238–242
34. http://www.shapa.co.uk/pdf/techdata.pdf. Accessed 17 October 2009